Polar Biol (2001) 24: 687–696
DOI 10.1007/s003000100269

ORIGINAL PAPER

Astrid U. Bracher · Max M. Tilzer

Underwater light field and phytoplankton absorbance in different surface water masses of the Atlantic sector of the Southern Ocean

Accepted: 2 April 2001 / Published online: 30 May 2001

Abstract Spectral water transparency and phytoplankton light absorbance were studied in the Atlantic sector of the Southern Ocean during the Southern Ocean JGOFS ANT XIII/2 cruise in early austral summer 1995/1996. The study area comprised three zones, which differed markedly with respect to their hydrographic and planktological characteristics: the Antarctic Polar Frontal Zone with adiatom bloom, the Antarctic Circumpolar Current outside frontal systems with phytoplankton-poor water and a higher flagellate abundance than in the other two areas, and the marginal ice zone with a *Phaeocystis* bloom. The influence of phytoplankton on spectral water transparency was assessed by two independent procedures: the pigment-specific beam absorption coefficient, $a_\phi^*[\lambda]$, at all stations, as estimated by spectroscopy of in vivo light absorption of plankton on glass fibre filters, and the pigment-specific light attenuation, ($k_c[\lambda]$), as derived by regression analysis of spectral in situ vertical light attenuation coefficients in the sea against concomitant pigment concentrations. Values of $a_\phi^*[\lambda]$ and vertical profiles of light attenuation by phytoplankton exhibited regional differences that corresponded with the three zones from which samples had been collected. These differences can be related to the specific characteristics of the three zones with respect to cell size distribution, pigment composition and biomass. The observed variations in $a_\phi^*[\lambda]$ values should be considered when oceanic primary production is to be estimated by biooptical modelling.

A.U. Bracher (✉) · M.M. Tilzer
Alfred-Wegener-Institute for Polar
and Marine Research, Postfach 120161,
27515 Bremerhaven, Germany

Present address: A.U. Bracher
University of Bremen, FB 1, Institute of Environmental Physics,
P.O. Box 330440, 28334 Bremen, Germany
e-mail: bracher@uni-bremen.de
Fax: +49-421-2184555

Present address: M.M. Tilzer
Aquatic Ecology, University of Constance,
78457 Konstanz, Germany

Introduction

The problem of spatial and temporal heterogeneity in the optical properties of water is crucial for the assessment of the large-scale distribution of biomass and primary production in the sea. This issue has been addressed by the definition of biogeochemical provinces, areas of the ocean in which the properties of the phytoplankton are consistent and can be predicted from a restricted suite of measurements (Platt et al. 1991).

The apparent optical property which combines the inherent optical properties of the ocean for a description of irradiance attenuation is the spectral diffuse attenuation coefficient, $k_d[\lambda]$. At any given wavelength, vertical light attenuation in natural water bodies can be ascribed to the water itself (k_w), non-algal material suspended and/or dissolved in the water, (k_g), and phytoplankton ($k_c[\lambda] \cdot$ [chl a + phaeo a]). Within a few percent, the magnitude of $k_d[\lambda]$, an apparent optical property, can be approximated by the ratio between the absorption coefficient $a(\lambda)$, an inherent optical property, and the mean cosine of irradiance field, μ (Priesendorfer 1976; Stavn 1988):

$$k_d[\lambda] = a[\lambda]/\mu \tag{1}$$

As an inherent property, $a[\lambda]$ can be written as the sum of its components parts:

$$a[\lambda] = a_w[\lambda] + a_s[\lambda] + a_d[\lambda] + a_\phi * [\lambda] \cdot [\text{chl}a + \text{phaeo}a] \tag{2}$$

where the subscripts w, s and d denote water, soluble constituents and detritus, respectively. The absorption by phytoplankton is represented as a product of specific absorption by phytoplankton, $a_\phi^*[\lambda]$, and the sum of chl a + phaeo a. Changes in species composition and its physiological condition affect the absorption properties of phytoplankton, and consequently the attenuation of underwater light. Up to now the extensive examination and quantification of the variations of specific absorption by phytoplankton, $a_\phi^*[\lambda]$, for natural assemblages at different spatial scales has been poor (Babin et al. 1993).

Although the importance of variations in $a_\phi^*[\lambda]$ has been recognised (Platt and Sathyendranath 1988), $a_\phi^*[\lambda]$ is often assumed to be constant for given areas in remote-sensing models of primary production (Platt and Sathyendranath 1988; Platt and Sathyendranath 1989; Morel 1991). Lewis et al. (1985) showed that the initial slope of the P versus I curve (α^*) has a large potential impact on error on estimates of areal primary production, α^* being the product of the maximal quantum yield of photosynthesis and the mean specific absorption coefficient weighted by the spectrum of the scalar irradiance between 400 and 700 nm.

With respect to its optical properties, the Southern Ocean is a poorly sampled region, although parameterisation of these properties is essential for the application of ocean-colour remote sensing of phytoplankton biomass and the estimation of primary production. Studies looking at the spectral composition of the underwater light field of the Southern Ocean have only been performed in the following areas: Antarctic Peninsula and Drake Passage (Stramski and Montwill 1982; Mitchell 1992; Fenton et al. 1994), Weddell Sea (Tilzer et al. 1994), Bellinghausen and Amundsen Seas (Stambler et al. 1997) and Ross Sea (Arrigo et al. 1998).

As a contribution to enhance the database that might be useful for the estimation of primary production in the Southern Ocean, we present here analyses of the first biooptical measurements obtained within the Atlantic sector. The spectral properties of the underwater light within the three investigated regions, the Antarctic Polar Front (APF), the Antarctic Circumpolar Current (ACC) outside of frontal systems, and the marginal ice zone (MIZ), show differences. These differences can be related to hydrological and biological factors, regarding photoadaptation and photoacclimation of the phytoplankton.

Materials and methods

During the Southern Ocean JGOFS cruise ANT XIII/2 aboard the RV Polarstern (Dec. 1995 to Jan. 1996), 24 stations were sampled within the Atlantic sector of the Southern Ocean (49–67°S and 6°W–12°). All stations were in the open water without any ice cover. In situ water samples were restricted to the uppermost 120 m of the water column.

Underwater light spectra

Vertical profiles of the downwelling spectral distribution of the underwater light field were measured using an MER-2040 underwater spectroradiometer equipped with a cosine receptor (Biospherical Instruments, San Diego). Within the PAR (photosynthetically available radiation: 400–700 nm) range, light was measured at wavelengths of 412, 443, 465, 490, 510, 520, 550, 560, 633, 665 and 683 nm (10 nm bandwidth). Thus the wavelengths which are measured by the SeaWiFS ocean colour satellite were included. In addition, two wavelengths within the UV-A range (340 and 380 nm) were measured. Changes in surface irradiance during the cast were recorded in parallel with the casts by an on-deck spectroradiometer (MER-2041), measuring as a reference at the same wavelengths as the underwater light meter. Special care was taken to avoid shading of the underwater spectroradiometer by the vessel during the casts. Dark values measured immediately after the cast with the instrument shielded from light within a flowing seawater tank were subtracted from the underwater readings.

Analysis of water samples

Measurements for light absorptions by particles and chlorophyll *a* concentrations were carried out using water sampled at six depths within the euphotic zone from a Bio-Rosette. The surface-water samples were taken with a bucket. At stations F4 and F6–F11, only surface-water samples were taken.

Chlorophyll data from the cruise were obtained from Hense et al. (1998) and Bracher et al. (1999). Chlorophyll and phaeophytin concentrations were analysed using the method of Evans et al. (1987), after filtering water samples onto Whatman GF/F filters and extracting the pigments by using 90% acetone. Determinations were performed by fluorometry of the extracts (Turner Design fluorometer) after grinding.

A volume of 1–2 l of water taken from the same depths as the pigment composition samples was filtered onto glass-fibre filters (GF/F Whatmann) for estimating light absorption by particles. Spectral absorption between 300 and 750 nm due to particles was measured with a double-beam spectrophotometer (Varian model cary 3). Before filtering the sample, filters had been well pre-soaked in filtered seawater. In order to correct for the individual attenuation properties of the filters used, their light attenuation was measured as a background correction prior to the filtration of the particle samples. A clean, wet filter was used as reference blank during all measurements, and baseline variations were automatically corrected for. All particulate absorption spectra were corrected for scattering by subtracting the optical density at 750 nm from the entire spectrum before calculating absorption (Kiefer and SooHoo 1982).

The particulate absorption coefficients ($a_p[\lambda]$, m^{-1}), corrections for detritus absorption ($a_d[\lambda]$, m^{-1}), and specific absorption coefficients of phytoplankton ($a_\phi^*[\lambda]$, m^2 mg chl a + phaeo a^{-1}) were determined by the method of Yentsch (1962), modified by Bricaud and Stramski (1990) using the β-correction of Mitchell and Kiefer (1988). The spectrally weighted mean absorption coefficient for PAR ($\bar{a}_\phi^*$, m^2·mg chl a + phaeo a^{-1}), a parameter weighted according to the spectral irradiance of the light source, was calculated using the equation of Atlas and Bannister (1980):

$$\bar{a}_\phi^* = \frac{\sum_{700}^{400} a_\phi^*[\lambda] \cdot E_d[\lambda]\Delta\lambda}{\sum_{700}^{400} E_d[\lambda]\Delta\lambda} \quad (3)$$

For definitions and dimensions of all symbols used, see Table 1.

By integrating irradiance fluxes in the 11 measured wavelengths, PAR at the discrete depth z, E_z[PAR], was estimated by assuming that they were valid for the entire waveband in whose mid-point irradiance was measured:

$$E_z[\mathrm{PAR}] = \Sigma E_z[\lambda]\Delta[\lambda] \quad (4)$$

Vertical attenuation coefficients of PAR, k_d[PAR], were determined from linear regression analysis of the natural logarithms of PAR versus depth by using 20 adjacent data points from discrete depths (5–100 m, 5 m-interval) for each determination. Correlations in these regression analyses were >0.99. The attenuation coefficient of PAR at the discrete depth z, k_d[PAR](z), was measured:

$$-k_d[\mathrm{PAR}](z) = \{\ln E_d[\mathrm{PAR}](z) - \ln E_d[\mathrm{PAR}](0)\}/z) \quad (5)$$

Attenuation coefficients of downwelling irradiance, $k_d[\lambda]$, were determined as k_d[PAR]. Data from the upper 5 m were not included in the calculation to avoid possible artefacts due to waves and ship shadow. According to the method of Smith and Baker (1978), the pigment-specific vertical light attenuation coefficient at λ, $k_c[\lambda]$, and also the k_c[PAR] values in the same way, were estimated from the slope of the regression line of $k_d[\lambda]$ as a function of chlorophyll concentration, using data from all stations; the y-intercept was interpreted as a measure of "background" light attenuation in the absence of any phytoplankton, due to water itself ($k_w[\lambda]$) and non-algal material (detrital particles and gilvin, $k_g[\lambda]$). The spectral specific vertical attenuation coefficients for sea water

Table 1 List of all symbols used in text

Symbol	Meaning	Unit
$a_p[\lambda]$	Particulate absorption coefficient at wavelength λ	(m^{-1})
$a_d[\lambda]$	Detritus absorption coefficient	(m^{-1})
$a_\phi[\lambda]$	Phytoplankton absorption coefficient	(m^{-1})
a_ϕ*[λ]	Pigment-specific absorption coefficient	(m^2·mg chl a^{-1})
$\bar{a}^*_\phi$	Spectrally weighted mean absorption coefficient	(m^2·mg chl a^{-1})
ACC	Antarctic Circumpolar Current outside of frontal systems	
APF	Antarctic Polar Front	
$E_d[\lambda]$	Downwelling irradiance	(μW cm^{-2})
$k_c[\lambda]$	Pigment-specific vertical light attenuation coefficient at λ	(m^2·mg chl $a^{-1)}$
k_d[PAR](z)	Light attenuation coefficient of PAR at depth z	(m^{-1})
$k_d[\lambda]$	Vertical light attenuation coefficient at wavelength λ	(m^{-1})
$k_g[\lambda]$	Vertical light attenuation coefficient due to non-algal material at λ	(m^{-1})
$k_w[\lambda]$	Vertical light attenuation coefficient due to water at λ	(m^{-1})
MIZ	Marginal Ice Zone	
μ	Mean cosine of irradiance field	
PAR	Photosynthetically available radiation from 400 to 700 nm	(μmol q·m^{-2}·s^{-1})
UML	Upper mixed layer depth	(m)
UV	Ultraviolet radiation from 280 to 400 nm	(μW cm^{-2})
z_{eu}	Euphotic depth, defined by the depth where underwater; PAR has decreased to 1% of the coincident surface value	(m)

$k_w[\lambda]$ were taken from Baker (1981) to derive k_g by difference ($k_g[\lambda] = k_d[\lambda] - k_w[\lambda] - k_c[\lambda] * [\text{chl}a + \text{phaeo}a]$).

Results

The three different zones, the Antarctic Polar Front, the Southern Antarctic Circumpolar Current outside frontal systems, and the Marginal Ice Zone were distinguished by their biological features, with respect to pigment composition (Bracher et al. 1999):

- the APF (49–51°S) was characterised by a diatom bloom of 0.15–2.4 mg chl *a* m^{-3} in the upper 40 m;
- the ACC (52–62°S) by scarce phytoplankton biomass with maxima of chlorophyll *a* concentration below 0.5 mg chl *a* m^{-3};
- the MIZ at the ice edge displayed a *Phaeocystis* bloom, maxima of chlorophyll *a* concentration above 2.4 mg chl *a* m^{-3}.

Station S30 was in the MIZ; stations F4, F6, S6, S8–S10, S14, S15 and S31 were in the ACC and the other stations (F7–F11, S13, S16, S18–S21, S25, S29, S32) were in the APF (Table 2).

The euphotic depth z_{eu} [PAR] ranged from 28 to 90 m. Stations within the ACC showed minimum values for k_d[PAR] and, consequently, maximum euphotic depths, whereas the stations of the APF showed highest values for k_d[PAR], especially at the centre of the phytoplankton bloom (stations S13, S21, S25, S29, S32). The station within the *Phaeocystis* bloom (station 30) also showed high values for k_d[PAR] (0.115 m^{-1}) and low values for z_{eu}[PAR] (40 m).

A regression analysis of vertical attenuation coefficients versus chlorophyll concentration yielded the following equation:

$$k_d[PAR] = 0.041 \cdot [chla + phaeoa] + 0.048$$

$$r^2 = 0.80,\ P < 0.001,\ n = 20.$$

The slope of the regression line has been used to estimate the chlorophyll-specific attenuation coefficient k_c[PAR]. The *y*-intercept corresponds to the attenuation caused by water and non-algal substances ($k_w + k_g$) (Fig. 1).

As observed previously (Tilzer et al. 1994) in phytoplankton-poor water such as encountered by us in the ACC, the most penetrating spectral region was in the blue range (Fig. 1b) and it shifted to green light, with maxima at 550 nm, when phytoplankton was abundant (Fig. 1a, c), as is typical for the APF and MIZ in our

Table 2 List of sampled stations during cruise ANT XIII/2 including position, date, time and zone. Stations were located in the Antarctic Polar Front (*APF*), the Antarctic Circumpolar Current (*ACC*) and the Marginal Ice Zone (MIZ) within the Atlantic sector of the Southern Ocean (*S* stations where samples were taken from the vertical profile; *F* stations where only surface samples were taken)

Station	Longitude	Latitude	Sampling date	Zone
S6	05.31	–50.22	09.12.95, 12.30 p.m.	ACC
S8	–03.13	–59.26	12.12.96, 11.00 a.m.	ACC
S9	–00.06	–53.60	22.12.96, 5.40 p.m.	ACC
S10	08.09	–50.29	25.12.96, 9.45 p.m.	ACC
S13	11.32	–49.54	29.12.96, 2.00 p.m.	APF
S14	11.32	–50.18	30.12.95, 3.00 a.m.	ACC
S15	11.31	–50.42	30.12.95, 9.00 a.m.	ACC
S16	10.17	–51.06	30.12.96, 6.00 p.m.	APF
S18	09.34	–50.42	05.1.96, 8.00 a.m.	APF
S19	09.34	–49.54	05.1.96, 11.45 p.m.	APF
S20	10.18	–49.30	06.1.96, 6.30 a.m.	APF
S21	10.18	–49.54	06.1.96, 3.30 p.m.	APF
S25	10.18	–50.18	07.1.96, 5.30 a.m.	APF
S29	10.18	–50.42	07.1.96, 11.00 p.m.	APF
S30	00.00	–63.40	16.1.96, 10.00 a.m.	MIZ
S31	05.50	–57.20	17.1.96, 4.30 p.m.	ACC
S32	11.33	–49.54	20.1.96, 6.00 a.m.	APF
F4	–05.08	–66.55	20.12.96, 5.00 a.m.	ACC
F6	–02.40	–61.46	21.12.96, 5.00 a.m.	ACC
F7	06.00	–50.42	24.12.96, 7.00 a.m.	APF
F8	10.24	–49.38	27.12.96, 7.00 p.m.	APF
F9	11.20	–49.41	01.1.96, 9.00 a.m.	APF
F10	10.50	–50.47	02.1.96, 11.00 a.m.	APF
F11	10.17	–49.50	03.1.96, 1.00 p.m.	APF

study. Attenuation in the red spectral range (< 660 nm) was mainly due to the water molecules themselves (Figs. 1, 2). Within the UV-A range, the attenuation coefficient for 340 nm (0.410 at station S30, 0.128 at S31) was higher than for 380 nm (0.227 at station S30, 0.076 at S31). We were able to detect irradiance at 340 nm down to 40 m and at 380 nm down to 64 m at station 31 (Fig. 3).

High correlations between pigment concentration and $k_d[\lambda]$ were obtained for wavelengths < 520 nm and at 560 nm (significant level < 0.001); at 550 and 633 nm correlations were lower (significant level < 0.01); no significance was found in the red (665 and 683 nm). The values of the pigment-specific attenuation coefficients, $k_c[\lambda]$, and the "background" light attenuation $k_w[\lambda] + k_g[\lambda]$ are presented in Table 3. Since every station was only measured once during the cruise and the comparison of k_d values and pigment concentrations of the same depths among stations would imply a larger error than a bulk analysis over the euphotic depth, one single value of $k_c[\lambda]$ and $k_g[\lambda]$ was estimated for all stations. By contrast, measurements of the pigment-specific absorption coefficient, $a_\phi^*[\lambda]$, were performed on individual samples and yielded differences between stations (Table 3).

From our data, we assessed the relative effects of the various components in influencing total attenuation of light over the spectrum of PAR. In Fig. 4, a chlorophyll-poor (in the ACC, station S31) and a chlorophyll-rich situation (in the APF, station S21 and in the MIZ, station S30) are compared. Regardless of phytoplankton abundance, attenuation of light in the red spectral range was dominated by the water itself, which transmits only little red light. In the blue spectral range, by contrast, light is efficiently attenuated by both photosynthetic pigments and non-algal material, but it was well transmitted by water molecules. At stationS30, ca. 45–85% and at station S21, ca. 45–70% of underwater light in the blue spectral range was absorbed by photosynthetic pigments while at station S31 only ca. 20–35% was absorbed. Other stations within the APF showed similar relative distribution patterns among the different spectral components, with a variability of +/-5% as compared to S21. The range of variability within the ACC was similar in comparison to S31.

Even when phytoplankton biomass does not vary with depth, pigment-specific absorption coefficients shift (Tilzer et al. 1994). This can be explained by the changes in the spectral composition of underwater light with depth. Figure 5 shows, according to the procedure of

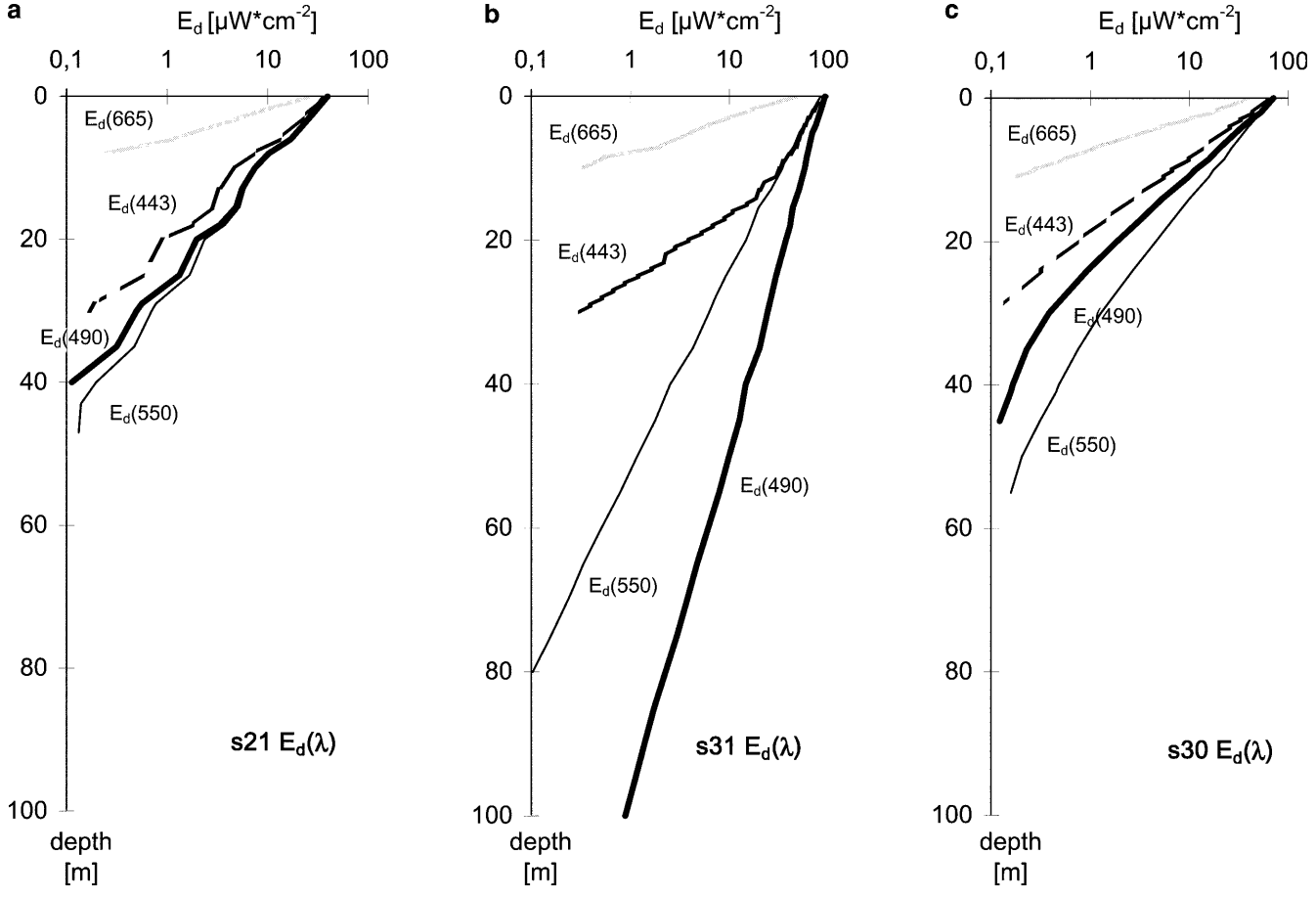

Fig. 1 Transmittance of downwelling irradiances ($E_d[\lambda]$) for 443 nm, 490 nm, 550 nm and 665 nm plotted semilogarithmically **a** for station S21 (within the APF), **b** for station S31 (within the ACC), and **c** for station S30 (within the MIZ)

Tilzer et al. (1994), the contributions of phytoplankton, water and non-algal material to the totat light attenuation coefficient of PAR at different depths. The constituents which are influencing the transparency showed a specific pattern for the stations of the three regions:

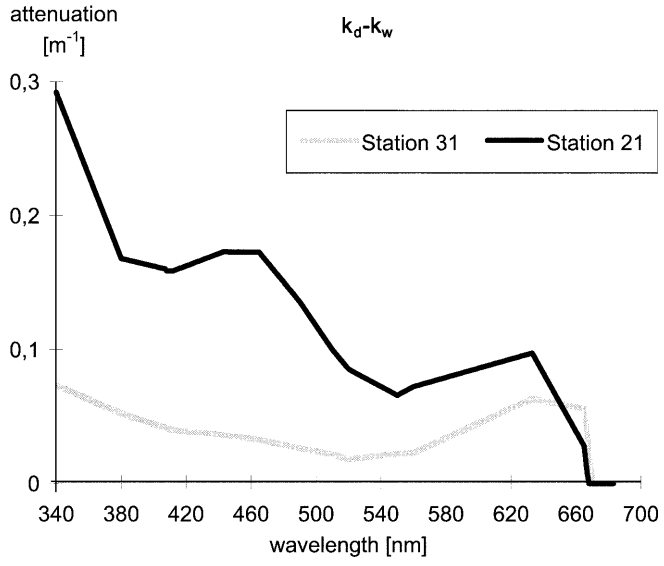

Fig. 2 Spectral attenuation coefficients due to all matter suspended and dissolved in the water at a phytoplankton-rich station (S21) and a phytoplankton-poor station (S31). Values were obtained by calculating the difference between the mean attenuation coefficient $k_d[\lambda]$ (determined by linear regression, for all values $P < 0.001$) and the attenuation coefficient of pure water $k_w[\lambda]$ (from Smith and Baker 1981)

1. In waters poor in phytoplankton (in the ACC), underwater irradiance with increasing depth was progressively restricted to the blue spectral range, because water was the main absorbing medium. As a consequence, the absorption by phytoplankton and by non-algal material increased with water depth (Fig. 5b) because the efficiency of light absorbed by both components in the blue range is high. There was a slight chlorophyll maximum in 60 m depth (0.46 μg chl *a*/l) as compared to values above (at 0–40 m, 0.24–0.31 μg chl *a*/l). However, since overall biomass was still low the increase in the contribution of phytoplankton to overall light attenuation with depth is mainly explained by shifting spectral composition of underwater light.
2. In waters within the APF, the contributions of the different components within the upper mixed layer varied little with depth except immediately below the surface. There is only a small near-surface maximum of absorption by phytoplankton in 15 m depth, corresponding with the maximum in chlorophyll concentration. Absorption by phytoplankton below the mixed-layer depth of about 35 m decreased sharply, as compared to values in shallower water (Fig. 5a).
3. In the MIZ, values of fractional light absorption by phytoplankton were high near the surface layer (0–15 m) where high biomass was found, and they dropped sharply below due to decreasing chlorophyll concentrations (Fig. 5c).

The regional differences in the spectral in vivo light absorption characteristics of phytoplankton $a_\phi^*[\lambda]$ were

Table 3 Different parameters that influenced the spectral water transparency in ANT XIII/2. Values of the pigment-specific vertical attenuation coefficient ($k_c[\lambda]$ in m^2 mg chl a^{-1}), the pigment-specific absorption coefficient ($a_\phi^*[\lambda]$ in m^2 mg chl a^{-1}), and the spectral attenuation coefficients for pure seawater $k_w[\lambda]$ and gilvin $k_g[\lambda]$ (both in m^{-1}). $k_w[\lambda]$ were taken from Smith and Baker (1978); $k_c[\lambda]$ were derived from the slope and $k_g[\lambda]$ from the *y*-intercept by difference $(k_g[\lambda] = k_d[\lambda] - k_w[\lambda] - k_c[\lambda] \cdot [\text{chl}a + \text{phaeo}a])$ of the regression line of $k_d[\lambda]$ as a function of chlorophyll concentration; estimations were based on $r^2 > 0.80$ and $P < 0.001$ at < 520 nm and 560 nm, and at 550 nm and 633 nm on $r^2 > 0.65$ and $P < 0.01$; no correlations were found for longer wavelengths. For all stations one $k_c[\lambda]$ and one $k_g[\lambda]$ value was calculated, which are mean values over the euphotic depth; $a_\phi^*[\lambda]$ was calculated for each individual station at six different depths and presented at 0 m and 30 m for the three different regions APF, ACC and MIZ. The statistical analyses (*t*-test) of $a_\phi^*[\lambda]$ data showed that $a\phi^*[\lambda]$ with λ = 412-510 nm were significantly higher ($P < 0.01$) at samples from the ACC than at samples from the APF

Wavelength (nm)	k_w	k_g	k_c	$a\phi^*$					
Zone, depth	for all stations over the euphotic zone			APF; 0 m	APF; 30 m	ACC; 0 m	ACC; 30 m	MIZ; 0 m	MIZ; 30 m
340	0.0660	0.0005*	0.133*	0.020–0.154	0.013–0.080	0.034–0.107	0.016–0.210	0.042	0.0195
380	0.0230	0.0178*	0.072*	0.007–0.043	0.007–0.020	0.012–0.024	0.013–0.037	0.016	0.012
412	0.0168	0.0308*	0.041*	0.012–0.026	0.011–0.026	0.030–0.036	0.027–0.034	0.025	0.017
443	0.0150	0.0232*	0.050*	0.015–0.035	0.013–0.033	0.041–0.050	0.032–0.045	0.033	0.021
465	0.0160	0.0169*	0.049*	0.014–0.034	0.012–0.030	0.040–0.049	0.029–0.043	0.034	0.021
490	0.0200	0.0117*	0.044*	0.010–0.025	0.008–0.023	0.029–0.036	0.025–0.029	0.023	0.015
510	0.0360	0.0090*	0.033*	0.006–0.015	0.005–0.015	0.016–0.021	0.011–0.018	0.014	0.009
520	0.0480	0.0059*	0.033*	0.005–0.011	0.004–0.011	0.011–0.015	0.008–0.013	0.011	0.008
550	0.0640	0.0146**	0.017**	0.002–0.005	0.001–0.005	0.004–0.006	0.003–0.008	0.004	0.004
560	0.0710	0.0082*	0.023*	0.001–0.004	0.001–0.003	0.001–0.004	0.002–0.007	0.001	0.002
633	0.3230	0.0231**	0.031**	0.003–0.006	0.002–0.005	0.006–0.007	0.004–0.009	0.006	0.005
665	0.4200	n.s.	n.s.	0.007–0.013	0.005–0.012	0.012–0.017	0.009–0.016	0.014	0.009
683	0.4530	n.s.	n.s.	0.006–0.013	0.005–0.012	0.012–0.017	0.008–0.016	0.015	0.009

*$P > 0.001$; **$P > 0.01$

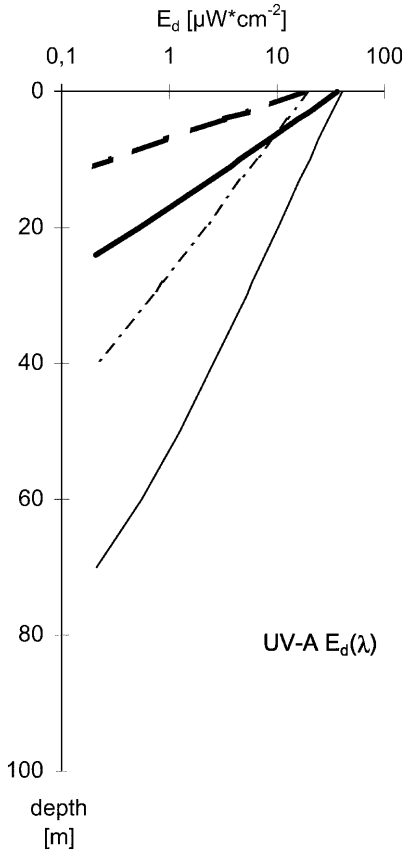

Fig. 3 Transmittance of downwelling irradiances ($E_d[\lambda]$) for 340 nm (*broken lines*) and 380 nm (*solid lines*) for station S30 (*thick lines*) and station S31 (*thin lines*)

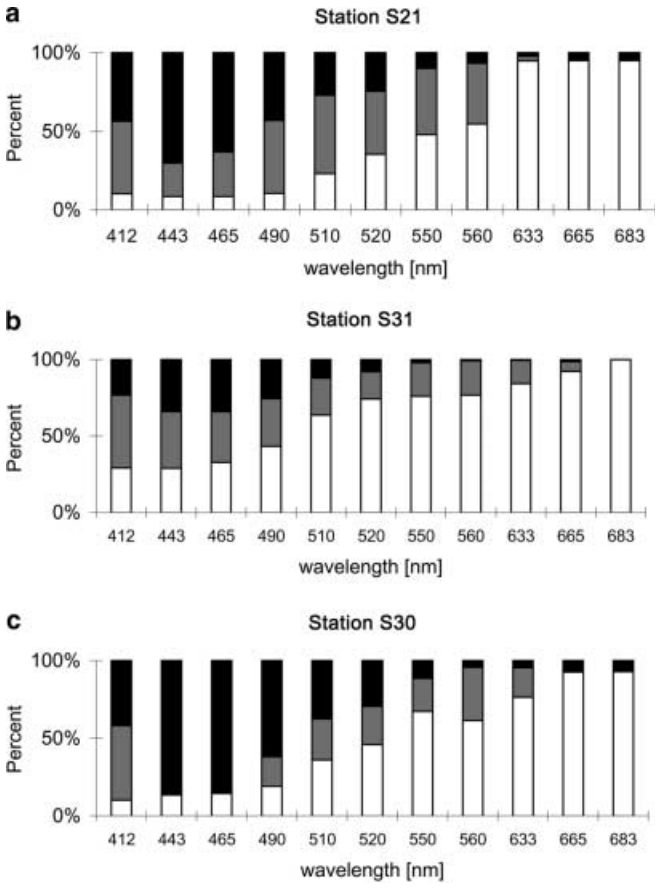

Fig. 4 Contributions of pure water (*white*), non-algal material (*grey*) and phytoplankton (*black*) to light attenuation as a function of wavelength at high (**a** station 21 with 122 mg chl *a* m^{-2} and **c** station S30 with 95 mg chl *a* m^{-2}) and at low (**b** station S31 with 29 mg chl *a* m^{-2}) phytoplankton biomass. For the attenuation by pure water, the values of Smith and Baker (1981) were used. For estimating attenuation by phytoplankton, specific absorption coefficients ($a_\phi^*[\lambda]$) were multiplied by pigment concentrations and divided by $\mu = 0.75$, an approximate estimate for the cosine of the irradiance field according to Bannister (1992). We based our estimates on $a_\phi^*[\lambda]$, rather than on $k_c[\lambda]$, because from $k_c[\lambda]$ we had only one value for all stations over the euphotic depth and no estimates in the red spectral range. Non-algal light attenuation was estimated by substracting values of attenuation by pure water and phytoplankton from total vertical attenuation coefficients $k_d[\lambda]$

analysed statistically by applying a *t*-test. Samples from surface waters and from 30 m depth were treated separately in order to be able to distinguish between the effects of differences in taxonomic composition and, also, shifts in phytoplankton photoacclimation. This analysis of the $a_\phi^*[\lambda]$ data showed that the samples from the ACC were significantly higher ($P < 0.01$) at $a_\phi^*[\lambda]$ with λ 412–510 nm than the samples from the APF (Table 3). The comparison of specific absorption by phytoplankton a_ϕ^* at different stations (Fig. 6) also shows that within the PAR range at station S31 (from the ACC), values are high as compared to the others, which is remarkable in the blue region (from 400 to 500 nm) and around 670 nm in the red spectral range (corresponding to chlorophyll *a* absorption peaks). Below-surface (Fig. 6a) values of station S30 (from the MIZ) were intermediate between the stations from the ACC and APF. At 30 m (Fig. 6b), the picture changes; station S21 (from the APF) shows higher a_ϕ^* values than station 30. In addition, data show that at stations S21 and S31, a_ϕ^* values varied little with depth, while at station S30 a_ϕ^* values for 0 and 15 m were considerably higher than at 30 m. In deep samples, differences between the regions were more pronounced than near the sea surface. In conclusion, both regional differences in species composition and vertical variability due to photoacclimation cause shifts in the spectra of pigment-specific light absorption. In both cases, shifting cellular pigment contents, both quantitatively and qualitatively, are the underlying cause.

Discussion

In order to assess the regional distribution of oceanic productivity, remote-sensing techniques have been applied, with great success (e.g. Plattet al. 1991). A generally accepted shortcoming of oceanic remote-sensing techniques is the fact that only information from near-surface waters can be collected. A second shortcoming that is less generally appreciated is the variability of the parameters on which primary productivity predictions are based. In this study, we demonstrate the wide re-

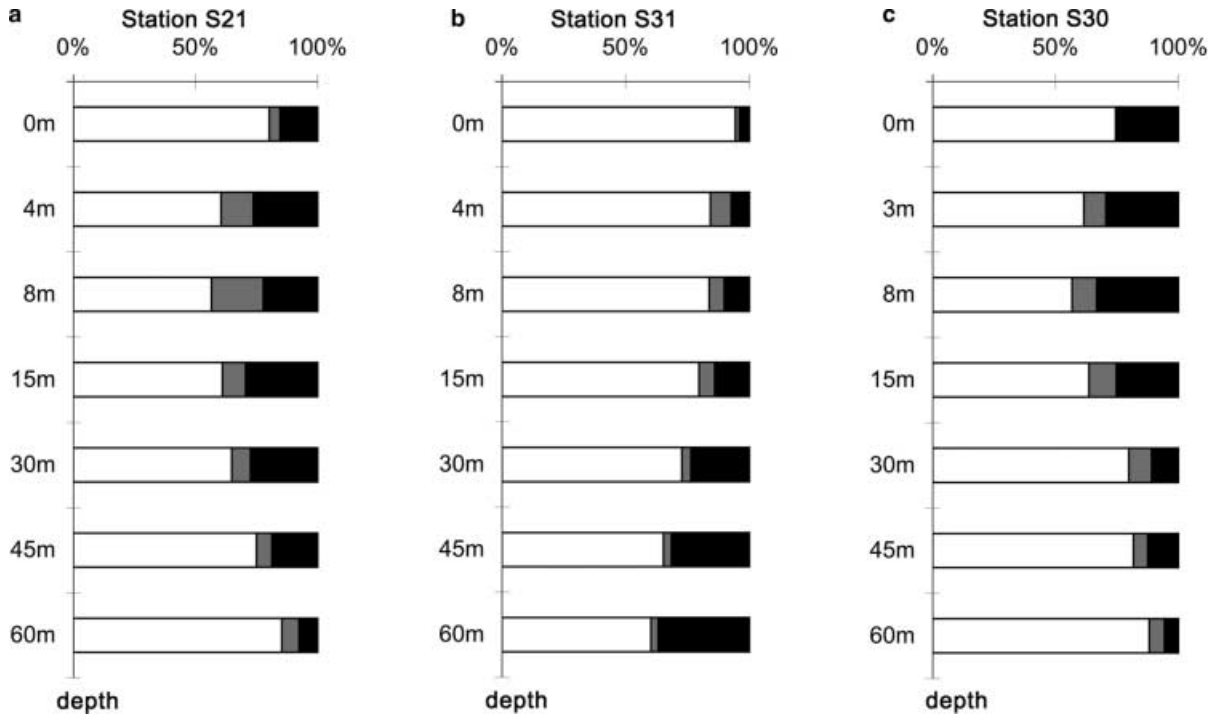

Fig. 5 Vertical profiles of the relative contributions of pure water (*white*), non-algal material (*grey*) and phytoplankton (*black*) to light attenuation of underwater PAR for station **a** S21 (within the APF), **b** S31 (within the ACC), and **c** S30 (within the MIZ). According to the procedure of Tilzer et al. (1994), the contributions of phytoplankton (through the depth-specific $\bar{a}^*_\phi$-value multiplied by pigment concentrations and divided by $\mu = 0.75$), water and non-algal material (both determined as in Fig. 4) to the light attenuation coefficient of PAR at depth z (k_d[PAR](z)) were determined

gional variability of the inherent optical properties of seawater and its dependence on total biomass and taxonomic composition of the phytoplankton assemblage. The efficiency at which photons entering the water column are harvested and utilised for photosynthesis by phytoplankton is a fundamental determinant of its productivity. Here we are able to show that this efficiency is variable, dueboth to light attenuation by non-algal material and to the inherent variability of the pigment-specific light absorption coefficient. Two fundamentally different methodological approaches have been used to determine pigment-specific light absorption coefficients, and yet models based on them rarely take into consideration these differences.

In this study, estimates of light absorption by phytoplankton are based on measurements using a spectrophotometer in the laboratory which yield inherent optical properties (a_ϕ*[λ]). By contrast, in most previous work the parameter $k_c[\lambda]$ was determined, which is based on field data and comprises both absorption and scattering. Moreover, in situ measurements are affected by the solar zenith angle. In this study, estimates of $k_c[\lambda]$ using the regression procedure of field data were only possible in the blue spectral range. However, these measurements do allow comparisons with a* at the respective wavelengths. As a rule k_c is ca. 25% higher than a*, owing to the above-mentioned methodological differences. Since a_ϕ*[λ] and $k_c[\lambda]$ depend on algal species composition and photoacclimation (Dubinsky 1992), these parameters can vary among stations. In our study, a_ϕ*[λ] values allow the assessment of these differences both between stations and between water depths within one single station (Table 3). Due to the limited number of data points available, only one regression analysis can usually be performed and one value of $k_c[\lambda]$ over a profile can be obtained. Moreover, $k_c[\lambda]$ includes the effects of detrital non-photosynthetic material, which frequently co-varies with chlorophyll. For all these reasons, for the interpretation of regional differences in biooptical characteristics of phytoplankton, a_ϕ*[λ] instead of $k_c[\lambda]$ values should be used.

Table 4 presents values for k_d[PAR] and $k_d[\lambda]$ previously measured within the Southern Ocean. Since in the studies of Stramski and Montwill (1982), Fenton etal. (1994), Stambler et al. (1997) and Arrigo et al. (1998) stations with high chlorophyll concentration (> 5 mg/m^3) were also found, the upper limit of the values was about a third higher than in our study and that of Tilzer et al. (1994). In contrast to this, our study, as well as that of Tilzer et al. (1994), were conducted far out in the open ocean. In the other studies, samples were also taken at the continental shelves. Overall, there is a problem in estimating correct k_d (and k_g) values above 600 nm. Because of the variation of $E_d(\lambda)$ by Raman scattering (Stavn and Weidemann 1988) and pigment fluorescence (Gordon 1979), the estimates of k_d can be smaller than the value of pure water. As Mitchell (1992) and Tilzer et al. (1994) pointed out, in the

Table 4 Comparison of k_d, $k_w + k_g$ (m^{-1}) *and* k_c (m^2 chl a^{-1}) values from cruise ANT XIII/2 (based on regression, for all $P < 0.001$) and the literature

Wavelength (nm)	Different wave length (nm) indicated with * or **	Stramski and Montwill (1982)	Fenton et al. (1994)	Fenton et al. (1994)	Tilzer et al. (1994)	Stambler et al. (1997)	Arrigo et al. (1998)	ANT XIII/2
		Drake P./S. Shetland Summer	South Georgia Early summer	Bransfield St. Late summer	Weddell Sea Spring	Bellingh. and Amund. Sea Late summer	Ross Sea Early summer	Atlantic sector Early summer
340						0.123–0.56		0.115–0.410
380						0.073–0.34		0.072–0.227
412	*425	0.049–0.300*				0.07–0.30	0.053–0.763	0.054–0.176
443			0.056–0.124	0.088–0.303	0.037–0.11	0.05–0.31	0.049–0.755	0.047–0.188
465		0.040–0.248				0.045–0.32		0.043–0.189
490						0.04–0.29	0.033–0.624	0.040–0.156
510						0.06–0.26	0.041–0.510	0.049–0.136
520	525*	0.070–0.175*	0.070–0.105	0.087–0.373		0.07–0.23		0.056–0.134
550	*535,**555	0.069–0.172*	0.075–0.131	0.099–0.313		0.08–0.2	0.073–0.298**	0.073–0.130
560	*580	0.131–0.215*			0.044–0.095	0.09–0.18		0.079–0.144
589	*596		0.113–0.148*	0.150–0.385*				
633	*620	0.250–0.481*				0.3–0.35		0.326–0.423
665			0.166–0.642	0.343–0.659		0.35–0.42	0.024–0.735	0.250–0.521
683		0.568–0.757			0.329–0.383	0.34–0.49		0.140–0.443
k_d[PAR]					0.044–0.131			0.051–0.161
k_c[PAR]					0.042	0.0680		0.041
$k_w + k_g$[PAR]					0.06			0.0476

Fig. 6 Spectra of (pigment-specific) absorption a_ϕ* at three representative stations: S21 for the APF, S31 for the ACC and S30 for the MIZ at **a** 0 m and **b** 30 m

Southern Ocean, concentrations of non-algal material are exceptionally small and derived mainly from autochthonous sources because terrestrial influx is virtually negligible.

Estimations of k_g in the Bransfield Strait yielded consistently higher values than those of Tilzer et al. (1994), Mitchell (1992) and Arrigo et al. (1998). Higher proportions of detritus were possibly present during the study of Fenton et al. (1994), which was performedin late summer when phytoplankton had begun to degrade. All other studies (Fig. 7a) were either performed in spring or early summer. Hense et al. (1998) showed that during our study the bloom at the APF was growing slowly, with minimal losses due to settling fluxes. Fresh phytoplankton blooms are generally characterised by a paucity of detritus (Sakshaug and Skjodal 1989). The later in the season, the lower the ratio of k_c to k_d and the higher k_g become. This difference is mainly seen in the blue spectral range.

Our estimates of k_c are in good agreement with those of Tilzer et al. (1994), but differ from those of Arrigo et al. (1998), Stambler et al. (1997) and Mitchell (1992) (Fig. 7b). Methodological differences, such as systematic

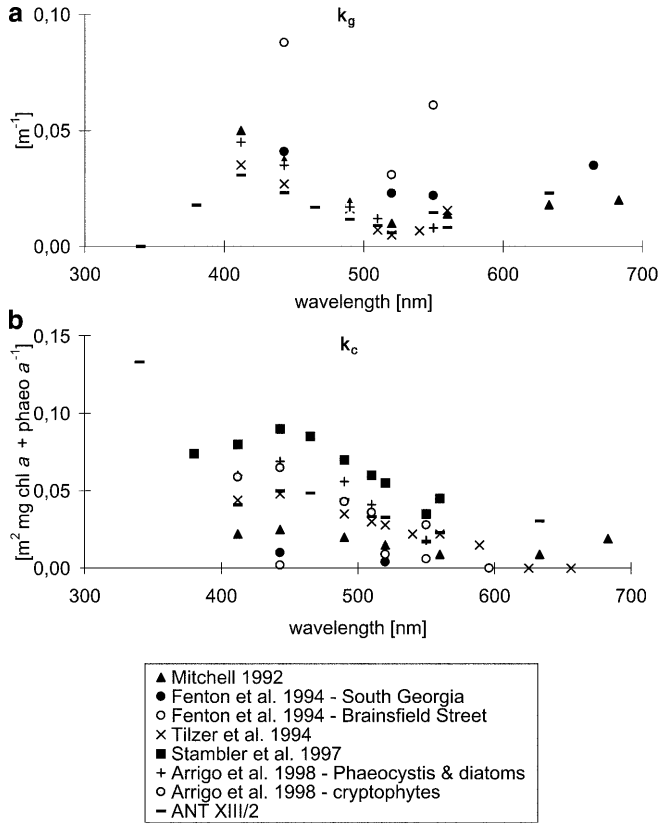

Fig. 7 Comparison of **a** k_g and **b** k_c values from the cruise ANT XIII/2 (estimations are based on $r^2 > 0.80$ at $P < 0.001$ at 560 nm, 520 nm, and shorter wavelengths, at 550 nm and 633 nm with $r^2 > 0.65$ at $P < 0.01$; no correlations were found for longer wavelengths) and the literature

errors occurring during the determination of chlorophyll concentrations, may also contribute to the variation of k_c values in the literature.

Variations in a_ϕ* from one algal species to another can be explained by differences in size, the type of other photosynthetic pigments present and their ratio to chlorophyll *a* due to the stage of photoacclimation. At low growth irradiances, phytoplankton increase the cellular pigment concentrations, thus intensifying the package effect (Mitchell and Kiefer 1988). The package effect is a function of particle diameter and, hence, cellular pigment content (Morel and Bricaud 1981). The cellular pigment content and the size of the photosynthetic units are increased in order to enhance the amount of photons intercepted, to improve overall the photosynthetic efficiency (Laws and Bannister 1980; Falkowski et al. 1985; Perry 1994). However, Mitchell and Kiefer (1988) suggested that fully shade-adapted cells may have a_ϕ* values 4 times lower than their high light-adapted counterparts. A large proportion of carotenoids, however, can increase the magnitude of a_ϕ*. Calculations for model cells having the same chlorophyll *a* content indicated that k_c for diatoms (probably a_ϕ* would be the same) would be about 70% higher than that for green algae because of the increased absorption in 500–560 nm due to fucoxanthin (Sathyendranath et al. 1987). One further possible cause of variation in the value of k_c, but not for a_ϕ*, from one species to another is the variation in their light-scattering properties due to the cell walls. Coccolithophorids and diatoms scatter light more intensely than algae without refractive integuments.

Low a_ϕ* values in the diatom and *Phaeocystis* blooms indicate pigment packaging, which is probably a result of the different size structure and photoacclimation within the phytoplankton communities. In our study, the bloom within the APF (> 0.8 μg/l) was dominated by particularly large, spiny and partly highly silicified diatoms (*Thalassiotrix* spp.), long chains of *Chaetoceros* spp. and *Pseudonitzschia* cf. *lineola* larger than 20 μm (Bracher et al. 1999). Large cells have lower pigment-specific absorption due to the package effect (Morel and Bricaud 1981). Here, more chlorophyll *a* per cell is encountered by photons, resulting in an overall decrease in absorption. In contrast, in the ACC, diatoms, dinoflagellates, prymnesiophytes and chrysophytes contributed more or less equally to the overall biomass, and the phytoplankton was dominated by the size class smaller than 20 μm (Bracher et al. 1999). Here, a_ϕ* values were much higher than in the other regions studied.

The upper mixed layer (UML) was shallow (10–15 m) at station 30 (within the MIZ) and around 35 m at station 21 (within the APF), while in the ACC outside of frontal systems UMLs exceeded 50 m (Strass et al. 1997). In the MIZ, the lower a_ϕ*[λ] values found at 30 m as compared to lower depths might be a result of the package effect. Below the UML, algae seem to be low light-adapted.

Our study was performed in case I waters (after Morel and Prieur 1977). In these waters, concentrations of material not correlated with chlorophyll *a* are low, and phytoplankton and their derivatives play a predominant role in determining the optical properties. The correlation of the vertical attenuation coefficients k_d (340) and k_d(380) to chlorophyll concentrations can be due to substances that co-vary with chlorophyll, such as detritus, yellow substances and mycosporine-like amino acids (MAA). MAAs have been measured in all samples from the cruise (Bracher and Wiencke 2000), and can also be the cause of high a_ϕ*[340] values among all samples from the upper depths (< 30 m).

Conclusions

Our data show that, within the polar region, the variability among k_d and a_ϕ* values is high. Waters in the Southern Ocean have rather low chlorophyll concentrations and little absorption by non-algal material. The calculation of k_c derived from chlorophyll concentration and k_d values can only give an approximation since many factors, like the contribution of non-algal substances, which are influenced by the chlorophyll concentration, are not taken into consideration. By definition, a_ϕ* explains much better the optical properties of a phytoplankton community. The regional dif-

ferences in absorption characteristics found in our study can be explained by differences in phytoplankton biomass, size, species composition and in photoacclimation stages due to UML depths. Field data of Bracher et al. (1999) showed an error made when assuming a constant specific absorption spectrum on daily primary production rates of 22–97%. The primary model of Babin et al. (1993) indicated that this errror can be as high as 24% at large scale; at small scale, it can reach 17%. The sensitivity of models of primary production by remotely sensed data should be tested for well-defined subareas of different a_ϕ* values for oceanographic systems which are allowed to vary in size and shape.

Acknowledgements The authors thank C. Bratrich, R. Lehmann, the crew and the captain of R.V. Polarstern and chief scientist V. Smetacek for their support during ANT XIII/2. We thank I. Hense and M. Lucas for chlorophyll analysis, U. Hoge for technical instruction with the MER and three anonymous reviewers for critical comments on the manuscript. This is AWI contribution number AWI-N10103.

References

Arrigo KR, Robinson DH, Worthen DL, Schieber B, Lizotte MP (1998) Bio-optical properties of the southwestern Ross Sea. J Geophys Res 103:21683–21695

Atlas D, Bannister TT (1980) Dependence of mean spectral extinction coefficient of phytoplankton on depth, water color and species. Limnol Oceanogr 25:157–159

Babin M, Therriault J-C, Legendre L, Condal A (1993) Variations in the specific absorption coefficient for natural phytoplankton assemblages: impact on estimates of primary production. Limnol Oceanogr 38:154–177

Bannister TT (1992) Model of the mean cosine of underwater radiance and estimation of underwater scalar irradiance. Limnol Oceanogr 37:773–780

Bracher AU, Wiencke C (2000) Simulation of naturally enhanced UV-radiation on photosynthesis of Antarctic phytoplankton. Mar Ecol Prog Ser 196:127–141

Bracher AU, Kroon BMA, Lucas MI (1999) Primary production, physiological state and composition of phytoplankton in the Atlantic sector of the Southern Ocean. Mar Ecol Prog Ser 190:1–16

Bricaud A, Stramski D (1990) Spectral absorption coefficients of living phytoplankton and nonalgal biogenous matter: a comparison between the Peru upwelling area and the Sargasso Sea. Limnol Oceanogr 35:562–582

Dubinsky Z (1992) The functional and optical absorption cross-sections of phytoplankton photosynthesis. In: Falkowski PG, Woodhead AD (eds) Primary productivity and biogeochemical cycles in the sea. Plenum Press, New York, pp 31–45

Evans CA, O'Reilly JE, Thomas JP (1987) A handbook for the measurement of chlorophyll *a* and primary production. Biological investigations of marine Antarctic systems and stocks (biomass), vol 8. Texas A & M University, College Station, Tex

Falkowski PG, Dubinsky Z, Wyman K (1985) Growth-irradiance relationships in phytoplankton. Limnol Oceanogr 30:311–321

Fenton N, Priddle J, Tett P (1994) Variations in bio-optical properties of the surface waters in the Southern Ocean. Antarct Sci 6:443–448

Gordon HR (1979) Diffusive reflectance of the ocean. The theory of its augmentation by chlorophyll *a* fluorescence at 685 nm. Appl Opt 18:1161–1166

Hense I, Bathmann U, Hartmann C (1998) Spiny phytoplankton – slowing down the Carbon Pump in the Southern Ocean? EOS Trans Am Geophys Union 79:89

Kiefer DA, SooHoo JB (1982) Spectral absorption by marine particles of coastal waters of Baja California. Limnol Oceanogr 27:492–499

Laws EA, Bannister TT (1980) Nutrient and light-limited growth of *Thalassiosira fluviatilis* in continuous culture, with implications for phytoplankton growth in the ocean. Limnol Oceanogr 25:457–473

Lewis MR, Warnock RE, Platt T (1985) Absorption and photosynthetic action spectra for natural phytoplankton populations: implications for production in the open ocean. Limnol Oceanogr 30:794–806

Mitchell BG (1992) Predictive bio-optical relationships for polar oceans and marginal ice zones. J Mar Syst 3:91–105

Mitchell BG, Kiefer DA (1988) Chlorophyll *a* specific absorption and fluorescence excitation spectra for light-limited phytoplankton. Deep Sea Res 35:639–663

Morel A (1991) Light and marine photosynthesis: a spectral model with geochemical and climatological implications. Prog Oceanogr 26:263–306

Morel A, Prieur L (1977) Analysis of variations in ocean color. Limnol Oceanogr 22:709–722

Morel A, Bricaud A (1981) Theoretical results concerning light absorption in a discrete medium, and applications to specific absorption of phytoplankton. Deep Sea Res 28:1375–1393

Perry MJ (1994) Measurements of phytoplankton absorption other than per unit of chlorophyll *a*. In: Spinrad RW, Carder KL, Perry MJ (eds) Ocean optics. Oxford Monographs on Geology and Geophysics, Oxford, pp 107–117

Platt T, Sathyendranath S (1988) Oceanic primary production. Estimation of remote sensing at local and regional scales. Science 241:1613–1620

Platt TC, Caverill C, Sathyendranath S (1991) Basin-scale estimates of oceanic primary production by remote sensing: the North Atlantic. J Geophys Res 96:15147–15159

Priesendorfer R (1976) Hydrologic optics. US Dept of Commerce, Washington, DC

Sakshaug E, Skjodal HR (1989) Life at the ice edge. Ambio 18:60–67

Sathyendranath S, Platt TC (1989) Computation of aquatic primary production: extended formalisms to include the angular and spectral distribution of light. Limnol Oceanogr 34:188–198

Sathyendranath S, Lazzara L, Prieur L (1987) Variations in the spectral values of specific absorption of phytoplankton. Limnol Oceanogr 32:403–415

Smith RC, Baker KS (1978) Optical classification of natural waters. Limnol Oceanogr 23:260–267

Smith RC, Baker KS (1981) Optical properties of the clearest natural waters (200–800 nm). Appl Opt 20:177–184

Stambler N, Lovengreen C, Tilzer MM (1997) The underwater light field in the Bellinghausen and Amundsen Seas (Antarctica). Hydrobiologia 344:41–56

Stavn RH (1988) Light attenuation in natural waters: Gershun's law, Lambert-Beer law and the mean light path. Appl Opt 20:2326–2327

Stavn RH, Weidemann AD (1988) Optical modeling of clear ocean light fields: Ramnan scattering effect. Appl Opt 27:4002–4011

Stramski D, Montwill K (1982) Light conditions in the Antarctic water of the Drake Passage and the South Shetland Islands region during summer 1981. Pol Polar Res 3:153–170

Strass V, Timmermann R, Fischer H, Hofmann M, Gwilliam P, Wischmeyer A (1997) CTD stations and water bottle sampling. Rep Polar Res 221:34–39

Tilzer MM, Gieskes WW, Heusel R, Fenton N (1994) The impact of phytoplankton on the spectral water transparency in the Southern Ocean: implications for primary productivity. Polar Biol 14:127–136

Yentsch CS (1962) Measurements of visible light absorption by particulate matter in the ocean. Limnol Oceanogr 7:207–217